Transverse momentum spectra of dileptons at NA60

Kevin Dusling and Ismail Zahed

Department of Physics & Astronomy, State University of New York,

Stony Brook, NY 11794-3800, U.S.A.

(Dated: February 2, 2008)

arXiv:hep-ph/0701253v1 30 Jan 2007

Abstract

Recently the NA60 collaboration has reported the transverse mass spectra of dimuons coming from In-In collisions at 158 GeV/A. The measured yields display a strong invariant mass dependence not typical of radial flow, suggesting that different sources contribute in different mass regions. We interpret the dimuon transverse mass spectra from an early thermalized partonic phase and hadronic phase constrained by the strictures of broken chiral symmetry. Each phase develops a specific transverse momentum dependence by hydrodynamical expansion. We show that a measurement of the momentum anisotropy at NA60 could provide information on the dominant emission source (hadronic or partonic) in the intermediate mass region $1.5 \leq M \leq 3.0$ GeV.

PACS numbers:

I. INTRODUCTION

The observed dileptons coming from heavy-ion collisions can provide useful information on the early stages of the collision since electromagnetic probes do not interact with the medium after they are produced. It is therefore hoped that observed dileptons and photons could possibly provide an unambiguous signal for the quark gluon plasma. However, in any collision, there is also a substantial contribution of dileptons coming from the hadronic phase. An understanding of the resulting hadronic yields can provide crucial information on modifications to electromagnetic spectral functions due to chiral symmetry restoration.

The recent NA60 experiment at the CERN SPS has measured the invariant mass spectrum of low-mass dimuon pairs [1, 2, 3] in In-In collisions. It was seen that a large excess remained after subtracting contributions from expected hadronic (the cocktail) decays. The remaining excess was examined by a number of groups [5, 6, 7, 8, 9] and was interpreted by a combination of thermal partonic and hadronic contributions with modifications to the spectral function due to finite temperature and baryon density.

Even though the spectral function directly gives the rate of dilepton production, the experimentally observed yield differs due to the fact that the rates must be convoluted over the full space-time history of the collision region having widely varying temperature, baryon density, chemical potential and flow velocity. In addition, contributions from an early partonic phase must be included.

The NA60 results for the invariant mass spectra are important for pinning down modifications to the spectral function at finite temperature and baryon density but do not provide any information on collective transverse flow as the spectra are Lorentz invariant (not taking into account the nontrivial acceptance at NA60). More recently the NA60 collaboration has released acceptance corrected transverse mass spectrum [4] of the resulting dimuon yields in different mass windows. It was found that the spectrum has a shape atypical of radial flow with a significant mass dependence suggesting that the different mass regions are populated by different sources.

In the following paper we continue the analysis in [5] and analyze the transverse mass spectra of the dimuons produced at NA60 using the same rate equations and hydrodynamic evolution. In section 2 we summarize the pertinent partonic and hadronic rates used. In section 3, we present our transverse spectra and elliptic flow predictions. Our discussion

and conclusion follows in section 4.

II. DILEPTON RATES

We now summarize the rate equations used for the analysis that was preformed in [5]. For the partonic contribution above a critical temperature $T_c \approx 170$ MeV we use the standard leading order $q\bar{q}$ result for massless quarks:

$$\frac{dR}{d^4q} = \frac{-\alpha^2}{12\pi^4}\frac{1}{e^{q^0/T}-1}\Big(N_C \sum_{q=u,d,s} e_q^2\Big)\Big[1+\frac{2T}{|\vec{q}|}\ln(\frac{n_+}{n_-})\Big] \tag{1}$$

where N_C is the number of colors, e_q the charge of the quarks, and $n_\pm = 1/(e^{(q_0 \pm |\vec{q}|)/2T}+1)$.

Below T_c we use the rate equations presented in [10, 11, 12] for a hadronic gas at finite temperature and baryon density which are constrained entirely by broken chiral symmetry

$$\frac{dR}{d^4q} = \frac{-\alpha^2}{3\pi^3 q^2}\frac{1}{1+e^{q^0/T}}(1+\frac{2m_l^2}{q^2})(1-\frac{4m_l^2}{q^2})^{1/2} \times\Big[-3q^2 \mathrm{Im}\mathbf{\Pi}_V(q^2) + \frac{1}{f_a^2}\int da \mathbf{W}_1^F(q,k) + \int dN \mathbf{W}_N^F(q,p)\Big] \tag{2}$$

where da and dN are the appropriate phase space factors for mesons and nucleons respectively as outlined in [5]. The term in square brackets is obtained after keeping terms to first order in an expansion of the thermal structure function in both meson and nucleon density. Through the use of three-flavor chiral reduction formulas the terms $\mathbf{W}_1^F(q,k)$ and $\mathbf{W}_N^F(q,p)$ can be expressed in terms of vacuum vector and axial spectral densities which are measured in e^+e^- annihilation, τ decays and photo-reactions on nucleons and nuclei.

The final contribution comes from the decay of vector mesons after freezeout. These dileptons will play a large role in the transverse momentum spectra in the mass region of the given meson. The main effect is to harden the transverse mass spectra as the decaying mesons at freezeout are coupled to the transverse flow of the medium and are therefore boosted to higher q_T. Since the contribution from the decay of freezeout vector mesons was not included in our first analysis [5], we discuss the rate equation and the integration over the freezeout surface in the appendix.

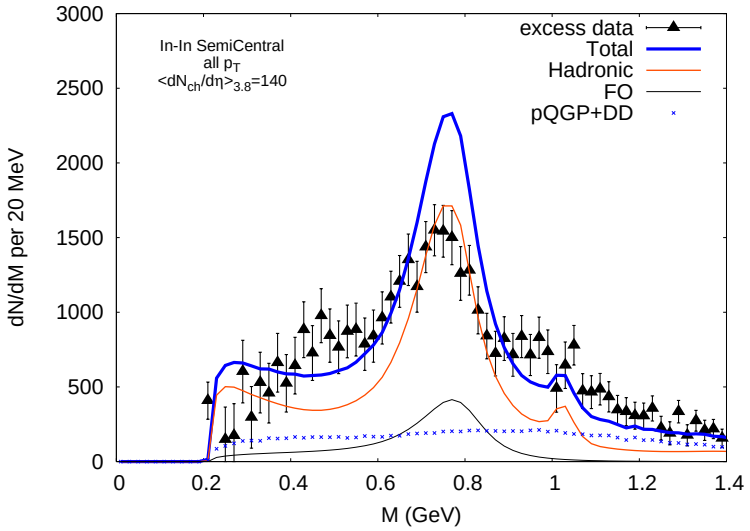

FIG. 1: Resulting dimuon yields after integration over the space time volume of the collision convoluted with a schematic acceptance of the NA60 experiment. Shown are the contributions from the perturbative QGP and charm decays (pQGP + $D\bar{D}$), the decay of freezeout ρ mesons (FO), and the thermal hadronic yields (Hadronic).

III. RESULTS

The rates outlined in the previous section were integrated over the space-time history of a full hydrodynamic simulation (details discussed in [5]) of the collision region at the CERN SPS collider. Shown in fig. 1 are the resulting invariant mass spectra (after a schematic acceptance of the NA60 detector was applied) compared to the data measured by the NA60 collaboration. The only difference from the analysis done in [5] is the inclusion of the freezeout contribution as shown in the figure. The net result is the same within %10 except for a small change in the overall normalization of the rates which can be accounted for by a decrease in the fireball freezeout temperature.

The data points in fig. 2 show the acceptance corrected transverse momentum spectrum of observed dimuon pairs after subtraction of the known hadronic cocktail (omitting the ρ) and charm contribution. The data was divided into three mass windows: a low mass region ($0.4 < \mathrm{M\ (GeV)} < 0.6$) below the ρ peak, a mass region around the ρ ($0.6 < \mathrm{M\ (GeV)} < 0.9$) and also a higher mass region ($1.0 < \mathrm{M\ (GeV)} < 1.4$). The data selection contains $dN_{ch}/d\eta > 30$ which corresponds to about $< dN_{ch}/d\eta > \approx 140$ which we use in the analysis.

The solid lines in fig. 2 show the results using the rates discussed in the prior section.

We show the contribution to the q_T spectrum from three sources: partonic (QGP), hadronic (Had) and freeze-out (FO) ρ contribution. The upper line in each figure shows the total yield.

Since a full hydrodynamic simulation of the collision is available we go one step further and calculate the elliptic flow of the produced dileptons [16] as is shown in fig 3 where $v2$ is a function of the invariant mass, transverse momentum and the impact parameter of the colliding system. The elliptic flow is defined as the weighted average of the yields with $\cos(2\phi)$:

$$v2(M, q_T) = \int d\phi \cos(2\phi) \frac{dN}{dM^2 dy q_T dq_T d\phi} / \int d\phi \frac{dN}{dM^2 dy q_T dq_T d\phi} \tag{3}$$

where ϕ is the angle between the dilepton momentum ($\vec{q}$) and the corresponding fluid element's velocity.

IV. DISCUSSION AND CONCLUSION

Our rates are overall consistent with the data in all mass regions. There is the possibility of some enhancement in the high q_T regions in both the low mass and medium mass regions. This could possibly be accounted for by fine tuning the freezeout temperature thereby increasing the freezeout ρ contribution and thus hardening the spectra in these mass regions. The drawback however, is that our yield around the rho is already about 30% above the measured yield. There is also some discrepancy in the low q_T regions, but as was pointed out in [20], one should not expect to explain this region by a thermal description only.

Based on the data, we feel that overall we have good control over the hydrodynamic evolution of both the temperature and flow velocity as well as the different source contributions (hadronic or partonic) in different mass regions. Of course with additional fine-tuning of fireball parameters (freeze-out temperature, etc.) it is possible to achieve better agreement, but we don't feel this is worth doing since the data is integrated over a wide range of centralities.

There has also been discussion whether the mass region above 1 GeV is dominated by partonic or hadronic radiation. Even though information on the source can be extracted from q_T spectra by looking at the effective temperature of the emission region as was done in [20] more information could be obtained if it was possible to measure the dilepton elliptic

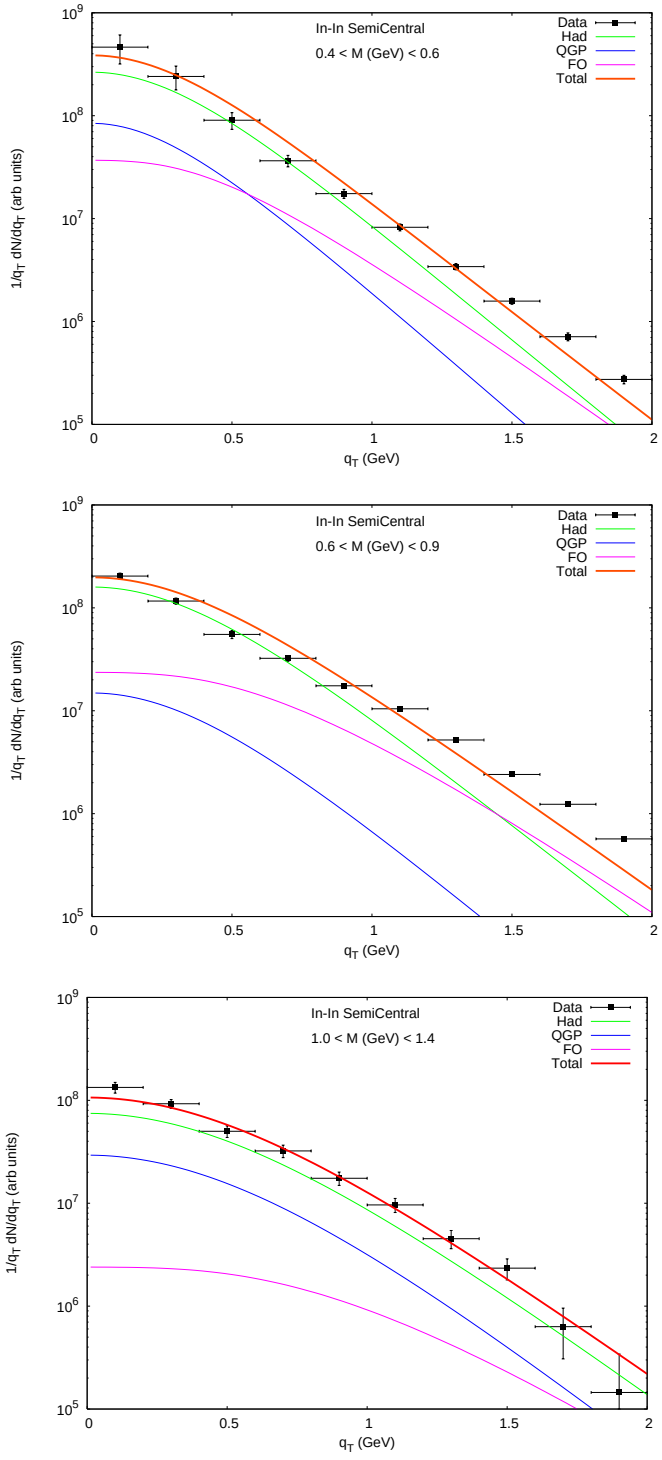

FIG. 2: (Color Online) Transverse momentum spectra for the three mass bins as measured by NA60. From top to bottom: $0.4 < \mathrm{M\ (GeV)} < 0.6$, $0.6 < \mathrm{M\ (GeV)} < 0.9$, $1.0 < \mathrm{M\ (GeV)} < 1.4$. The solid lines are our results including contributions from the partonic phase (QGP), hadronic phase (Had) and vacuum decays after freezeout (FO).

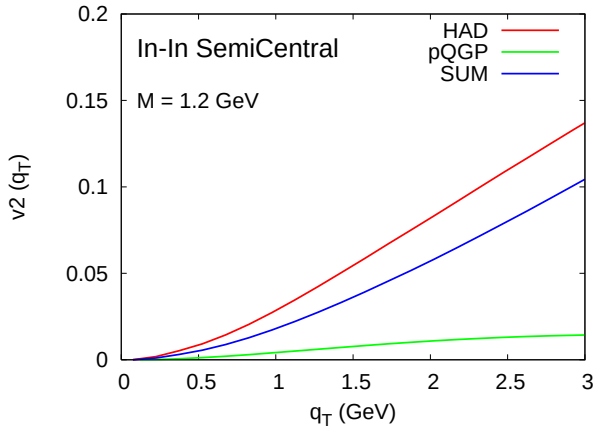

FIG. 3: (Color Online) Dilepton elliptic flow as a function of q_T for semi-central In-In collisions.

flow in various mass windows. Since the thermal partonic radiation is emitted early on from the collision region, one does not expect a large momentum anisotropy to have developed and therefore one would expect a much lower elliptic flow from dileptons coming from this region. On the other hand, hadronic radiation is emitted much later on and any momentum anisotropy would also be carried by the emitted dileptons.

In our rate calculations we find that in the $1.0 < \mathrm{M\ (GeV)} < 1.5$ region the dilepton contribution comes from both the hadronic and partonic phases. The hadronic yields in this mass region comes from contributions of both the axial spectral density which enters the rates from the chiral reduction formula due to chiral symmetry restoration by matter and also from the high energy tail of the vector spectral weight, part of which is from 4-π annihilation. In fig. 3 we show our calculated $v2$ from the partonic and hadronic yields. We also show the total $v2$, which is a weighted average of the two sources. One can see that depending upon the dominant emission source that qualitatively different elliptic flow develops at larger q_T.

To summarize: We have interpreted the dimuon transverse mass spectra as measured by the NA60 collaboration as coming from an early thermalized partonic phase as well as a hadronic phase constrained entirely by broken chiral symmetry, both of which develop specific transverse momentum dependence following the underlying hydrodynamic flow. After convolution of the rates over a hydrodynamic simulation of the conditions at the CERN SPS experiment we find good agreement between the resulting yields and the measured data. We show that a measurement of the momentum anisotropy at NA60

could provide information on the dominant emission source (hadronic or partonic) in the intermediate mass region $1.5 \leq M \leq 3.0$ GeV.

Acknowledgments.

We would like to thank Sanja Damjanovic, Edward Shuryak and Hans Specht for useful discussions. This work was partially supported by the US-DOE grants DE-FG02-88ER40388 and DE-FG03-97ER4014.

APPENDIX A: DILEPTONS AFTER FREEZE-OUT

We discuss how the dilepton rates from vector mesons decaying after freezeout was evaluated in the above result. A number of works [17, 18, 19] discuss this topic but it is presented here as well for completeness.

The contribution to the dilepton spectrum from decaying vector mesons at freezeout is given by:

$$\frac{dN}{dM^2\ d^3q/q^0} = \sum_V \frac{1}{\Gamma_V^{tot}} \frac{d\Gamma_{V\to\mu^+\mu^-}}{dM^2} E\frac{d^3N_V}{d^3p}\delta^4(p-q) \tag{A1}$$

In the above equation p is the momentum of the decaying vector meson V, $q = l_1 + l_2$ is the momentum of the dilepton pair and $M = \sqrt{l_1^2 + l_2^2}$ is the invariant mass of the dilepton pair. The quantity $E\frac{d^3N_V}{d^3p}$ is the number of vector mesons with momentum $\vec{p}$ and energy E at freezeout and can be evaluated using the Cooper-Frye [14] formula

$$E\frac{d^3N}{d^3p} = \frac{g}{(2\pi)^3}\int_\sigma f(q_0,T)p^\mu d\sigma_\mu \tag{A2}$$

The Cooper-Frye formula requires integration over σ, which is the four-dimensional space-time boundary. We show how this integration was done for a boost invariant, azimuthally symmetric expansion.

The quantity $d\sigma_\mu$ is the normal vector to the surface of the four-dimensional space-time volume set in our case by the freeze-out temperature $T_{f.o.}$ and is given by

$$d^3\sigma_\mu \equiv -\epsilon_{\mu\nu\lambda\rho}\frac{\partial\sigma^\nu}{\partial u}\frac{\partial\sigma^\lambda}{\partial v}\frac{\partial\sigma^\rho}{\partial w}du\ dv\ dw \tag{A3}$$

where u,v,w are three independent coordinates used to parameterize the hypersurface. Following [15] the four volume of the collision region is expressed as

$$\sigma^{\mu}(\tau, r, \phi, \eta) = [\tau \cosh\eta, r\cos\phi, r\sin\phi, \tau\sinh\eta] \tag{A4}$$

where $\eta = \frac{1}{2}\ln\frac{t+z}{t-z}$ is the spatial rapidity and $\tau = \sqrt{t^2 - z^2}$ is the proper time. Also for a boost invariant expansion, the vector meson's four momentum can be expressed as:

$$p^{\mu} = [m_{\perp}\cosh y, p_{\perp}\cos\phi^{p}, p_{\perp}\sin\phi^{p}, m_{\perp}\sinh y] \tag{A5}$$

where $m_{\perp} = \sqrt{M^2 + p_{\perp}^2}$ and y is the longitudinal rapidity.

Choosing to parameterize the freezeout hypersurface with coordinates (u,v,w)=(r,ϕ,η) the freezeout volume is:

$$\sigma_f^{\mu}(r, \phi, \eta) = [\tau_f(r)\cosh\eta, r\cos\phi, r\sin\phi, \tau_f(r)\sinh\eta] \tag{A6}$$

The subscript f in the above equation refers to the quantity at freezeout. Therefore σ_f^{μ} should be thought of as a parameterization of the space-time volume where freezeout occurs, or more precisely in our case the space-time volume having temperature $T = T_{f.o.}$. The fact that the freezeout proper time depends only on the fireball radius is due to the assumed boost-invariance and azimuthal symmetry. Using A3 we obtain

$$d^3\sigma_{\mu} = \Big(\cosh\eta, -\frac{\partial\tau}{\partial r}\cos\phi, -\frac{\partial\tau}{\partial r}\sin\phi, -\sinh\eta\Big)\tau r dr d\phi d\eta \tag{A7}$$

for the normal vector to the hypersurface.

Using the above expressions for p^{μ} and $d\sigma_{\mu}$ and performing the integration of Eq. A2 over the freezeout hypersurface, the total number of dileptons produced from decaying ρ mesons per unit four momentum is given as:

$$\frac{dN}{d^4q} = \int_0^{r_{f.o.}} dr \int_{-\infty}^{+\infty} d\eta \int_0^{2\pi} d\phi\ \tau r \times \Big[m_{\perp}\cosh(y-\eta) - \frac{\partial\tau}{\partial r}p_{\perp}\cos(\phi - \phi^{p})\Big]\frac{1}{\Gamma_{\rho}^{tot}}\frac{d\Gamma_{\rho\to\mu^+\mu^-}}{dM^2}\frac{g}{(2\pi)^2}f(p_{\mu}u^{\mu}, T) \tag{A8}$$

where we have chosen to orient the azimuthal angle ϕ with the direction of the fluid velocity and $f(p_{\mu}u^{\mu}, T)$ is the Bose distribution with $p_{\mu}u^{\mu} = m_{\perp}\gamma_{\perp}\cosh(y-\eta) - p_{\perp}u_{\perp}\cos(\phi - \phi^{p})$. The explicit form for the meson spectral function is given using the Breit-Wigner parameterization:

$$\frac{d\Gamma_{\rho\to\mu^+\mu^-}}{dM^2} = \Gamma_{\rho\to\mu^+\mu^-}\frac{1}{\pi}\frac{m_\rho\Gamma_\rho^{tot}}{(M^2-m_\rho^2)^2+(m_\rho\Gamma_\rho^{tot})^2} \tag{A9}$$

[1] S. Damjanovic *et.al.*, Nucl. Phys. A **774**, 715-718 (2006). arXiv:nucl-ex/0510044

[2] S. Damjanovic, arXiv:nucl-ex/0609026;

[3] M. Floris *et.al.*, arXiv:nucl-ex/0606023

[4] S. Damjanovic *et.al.*, arXiv:nucl-ex/0701015

[5] K. Dusling, D. Teaney, and I. Zahed, arXiv:nucl-th/0604071

[6] T. Renk and J. Ruppert, arXiv:hep-ph/0603110; arXiv:hep-ph/0605130

[7] H. van Hees and R. Rapp, arXiv:hep-ph/0603084; arXiv:hep-ph/0604269

[8] R. Rapp, H. van Hees and T. Strong, arXiv:hep-ph/0611339

[9] V.V. Skokov and V.D. Toneev, Phys. Rev. C **73** (2006) 021902.

[10] J. V. Steele, H. Yamagishi, and I. Zahed, Phys. Lett. B **384** (1997) 255.

[11] J. V. Steele, H. Yamagishi, and I. Zahed, Phys. Rev. D **56** (1997) 5605; Nucl. Phys. A **638** (1998) 495c.

[12] C. H. Lee, H. Yamagishi, and I. Zahed, Phys. Rev. C **58** (1998) 2899.

[13] Z. Huang, Phys. Lett. B **361**, 131 (1995).

[14] E. Cooper, G. Frye, Phys. Rev. D **10**, 186 (1974)

[15] J. D. Bjorken, Phys. Rev. D **27**, 140 (1983).

[16] U. Heinz, R. Chatterjee, E. Frodermann, C. Gale, and D. K. Srivastava, arXiv:nucl-th/0610014.

[17] B. Kampfer, O.P. Pavlenko, Eur. Phys. J. A10 (2001) 101-107. arXiv:nucl-th/0011021

[18] U. Heinz, K. S. Lee, and E. Schnedermann, Quark Gluon Plasma, editor: R. C. Hwa, World Scientific, Singapore, 471 (1990).

[19] P. V. Ruuskanen, Quark Gluon Plasma, editor: R. C. Hwa, World Scientific, Singapore, 519 (1990).

[20] Thorsten Renk and Jorg Ruppert, arXiv:hep-ph/0612113